CASE REPORT

Diagnostic challenges in vacuolar myelopathy: a didactic case report

Florian Ernst[1,2], Fritz Klausner[3], Waltraud Kleindienst[1,2], Heinrich Bartsch[1], Ninon Taylor[4] and Eugen Trinka[1,2]

INTRODUCTION: Because of the diagnostic complexity and potential pitfalls in interpreting test results, HIV-vacuolar myelopathy (HIVM) is far more often diagnosed postmortem than *in vivo*. In the era of highly active antiretroviral therapy (HAART), the topic of neuro-AIDS has become increasingly important. This case report covers some of the diagnostic problems encountered in vacuolar myelopathy based on magnetic resonance imaging (MRI) fiber-tracking pictures of the spine in a patient with HIVM, including a 1-year follow-up.
CASE PRESENTATION: A 49-year-old man felt progressive weakness, and difficulties while walking, and he suffered from incomplete voiding. A week before admission, follicles appeared on the right side of his neck and shoulder. His medical history included a chronic HIV infection treated with HAART and a B-cell lymphoma in complete remission after chemotherapy. The initial exam revealed thoracic hyposensitivity level distal to dermatome Th9, spastic paraparesis of the lower limbs and herpes zoster infection in dermatome C3/C4. A lesion of the thoracic myelon could be ruled out in the MRI scan, chemotherapy-induced polyneuropathy was stable, and no acute opportunistic infection of the CNS was found. HIV load in cerebrospinal fluid (CSF) was markedly elevated. An HIV-associated vacuolar myelopathy was diagnosed, revealing the HIV itself as etiology.
DISCUSSION: A negative or unspecific MRI scan excludes possible other causes, but by no means rules out HIV-related myelopathy. Furthermore, peripheral and central viral load should always be assessed to avoid missing a possible 'CSF HIV-escape'.

Spinal Cord Series and Cases (2016) **2,** 16020; doi:10.1038/scsandc.2016.20; published online 15 September 2016

INTRODUCTION

About 2 months before admission, a 49-year-old man felt a progressive weakness, and walking became increasingly difficult. He tumbled repeatedly, and mobility at home was possible only by supporting himself with his arms on furniture or by using a wheeled walker. Furthermore, he suffered from incomplete voiding. A week before admission, vesicles appeared on the right side of his neck and shoulder. He was sent to a neurological rehabilitation center with the diagnosis of a chemotherapy-induced polyneuropathy with sensory ataxia. There the initial neurological examination revealed a thoracic spinal-level hyposensitivity distal to dermatome Th9 and a spastic paraparesis of the lower limbs with positive spontaneous Babinski's sign on both sides. His medical history included (Figure 1a) the following: current herpes zoster (right dermatoma C3/C4), HIV-/Hepatitis B co-infection (diagnosed 9 months ago), voiding dysfunction (since 2 months) with an indwelling catheter, urinary tract infection (diagnosed 2 days before) and diffuse large B-cell lymphoma in complete remission (Stadium IVb with disseminated hepatic, localized gastric and 10% bone marrow affection at presentation; full remission after three cycles of rituximab, etoposide, doxorubicine, vincristine, cyclophosphamide and prednisolone—altogether eight cycles; vincristine was excluded after the fourth cycle because of worsening of polyneuropathy; prophylactic intrathecal cytarabine application three times—last application 7 months ago).

Alongside an antiretroviral therapy with emtricitabin, tenofovir and raltegravir since HIV was first diagnosed, his current medication included aciclovir (day 2), ciprofloxacin (day 2), gabapentin and vitamin B1/B6/B12 complex.

CASE PRESENTATION

First, a lesion of the thoracic myelon was considered. In the light of the rather complex medical history of this patient, an intraspinal expansive lesion, a para-/infectious myelitis or a paraneoplastic myelopathy seemed possible. Second, the pronounced progressive polyneuropathy reminded one of a Guillain–Barré syndrome or a chronic inflammatory demyelinating polyneuropathy, leaving behind the fact of the thoracic hyposensitivity level distal to the dermatome Th9. Furthermore, a progressive multifocal leukoencephalopathy also came into consideration, whereas a chemotherapeutic-induced myelopathy or an HIV-associated transverse myelitis seemed to be rather unlikely when considering the symptom chronology as well as former therapies. Funicular myelosis could be excluded because of the ongoing vitamin B substitution. Owing to the lack of pain, HAART-associated spinal epidural lipomatosis as differential diagnosis would have been an unlikely and extremely rare condition. Apart from qualifying AIDS activity, the next important diagnostic step was a magnetic resonance imaging (MRI) including a contrast agent investigation of the whole neuro-axis, electrophysiologic investigation and a lumbar puncture as well.

[1]Department of Neurology, Paracelsus Medical University Salzburg, Salzburg, Austria; [2]Spinal Cord Injury and Tissue Regeneration Center Salzburg (SCITReCS), Salzburg, Austria; [3]Division of Neuroradiology, Paracelsus Medical University Salzburg, Salzburg, Austria and [4]Department of Internal Medicine III with Hematology, Medical Oncology, Hemostaseology, Infectious Diseases, Rheumatology, Oncologic Center, Laboratory of Immunological and Molecular Cancer Research, Paracelsus Medical University Salzburg, Salzburg, Austria.
Correspondence: F Ernst (f.ernst@salk.at)
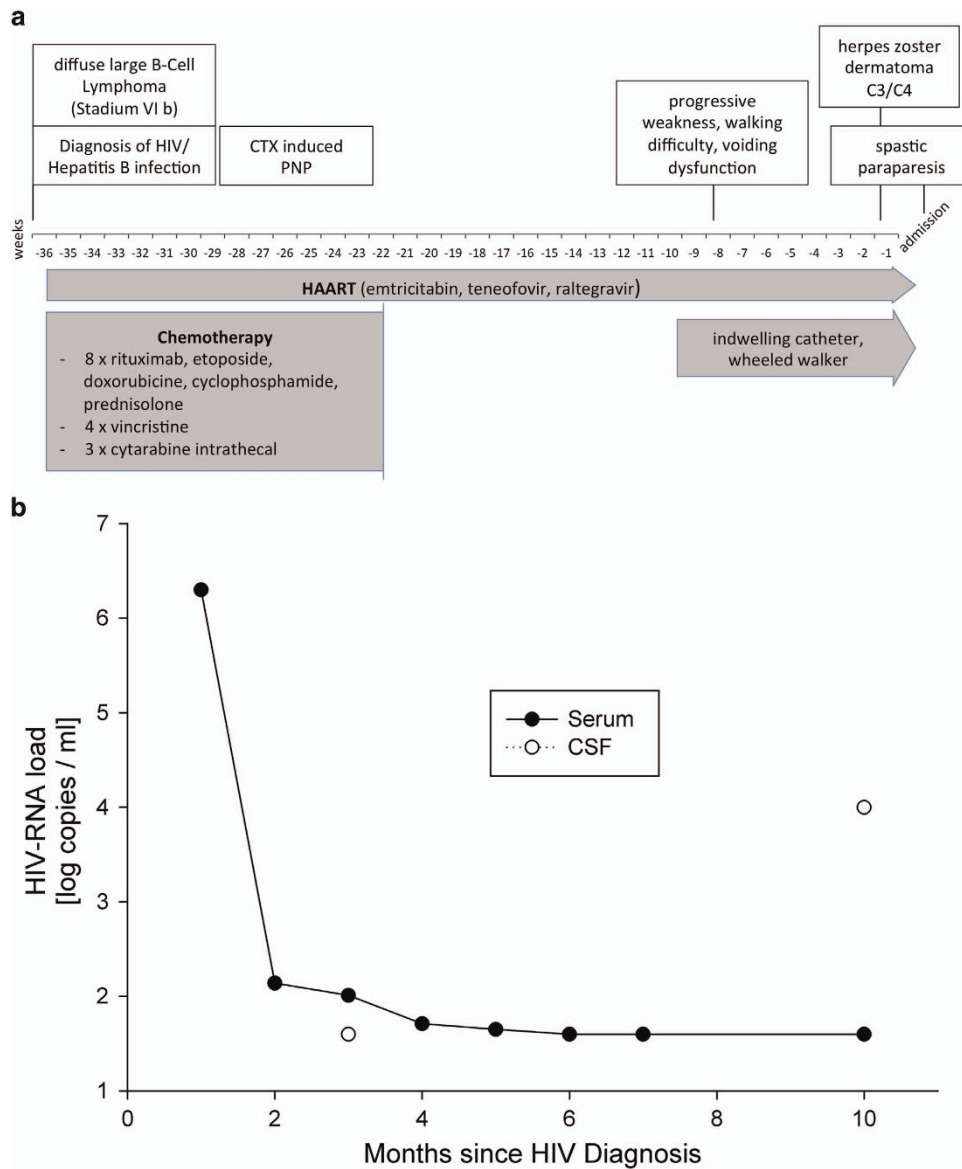
Figure 1. (a, b) Course of the disease with serum and CSF HIV-RNA load. (a) The timeline of diagnoses, therapies and symptoms. The patient underwent regular checks in the outpatient clinic for infectious diseases, where HIV-RNA load was measured in serum. After the start of HAART, the viral load dropped significantly below the detection limit. The CSF viral load was measured once at the time point of HIV diagnosis and the second time when the patient was admitted to our department. A clear heightened viral load in CSF can be seen as a possible 'CSF HIV-escape' (b).

Cerebral MRI merely showed discrete signs of leukoencephalopathy but no contrast agent enhancement, whereas spinal MRI revealed a reduced bone marrow signal without myelopathy signal and without contrast agent enhancement. The cervical and the thoracic cord of our patient appeared atrophic with an anteroposterior diameter of 5–6 and 4–5 mm, respectively. On the sagittal T2 images, no definitive hyperintense areas were visible (Figures 2a–d and 3a). CSF proteins and cell count were within normal ranges. Forty-five CD4+ and 408 CD8+ cells per µl (ratio 0.11) showed their nadir since the time point of HIV diagnosis, reflecting a critical peripheral immune status. Electroneurography showed mild improvement of the previously diagnosed mixed sensory accentuated polyneuropathy, and electromyography confirmed the chronic muscular neurogenic changes. Tibial nerve somatosensory-evoked potentials (SSEPs) confirmed the peripheral pathology, whereas medianus nerve SSEPs showed a slight peripheral slowing down without impairment of spino-thalamico-cortical tracks. The neuropsychological tests revealed slight deficits in learning ability (VLMT—verbal learning and memory test; subcategories learning performance and free recall) and cognitive performance (trail marking test), whereas verbal memory, memory of learned material, recognition ability, intelligence, attention and divided attention, and fear and depression (VLMT—subcategories consolidation and recognition; MMSE—mini mental state exam; WIE—Wechsler Intelligence Test; TAP—subtests go/nogo; HADS—Hospitaly Anxiety and Depression Scales) were just within normal ranges.

The absence of a space-occupying lesion or signs of myelopathy in the MRI required further reflection. Taken together, the results of the neuropsychological tests and the absence of typical cerebral lesions argued against progressive multifocal leukoencephalopathy, confirmed by the negative results of JC virus (John Cunningham virus) testing. Admittedly, for a middle-aged man with a higher educational level, the slight subclinical cognitive deficits were suspicious and pointed toward an intellectual impairment with no clear etiology at the moment,
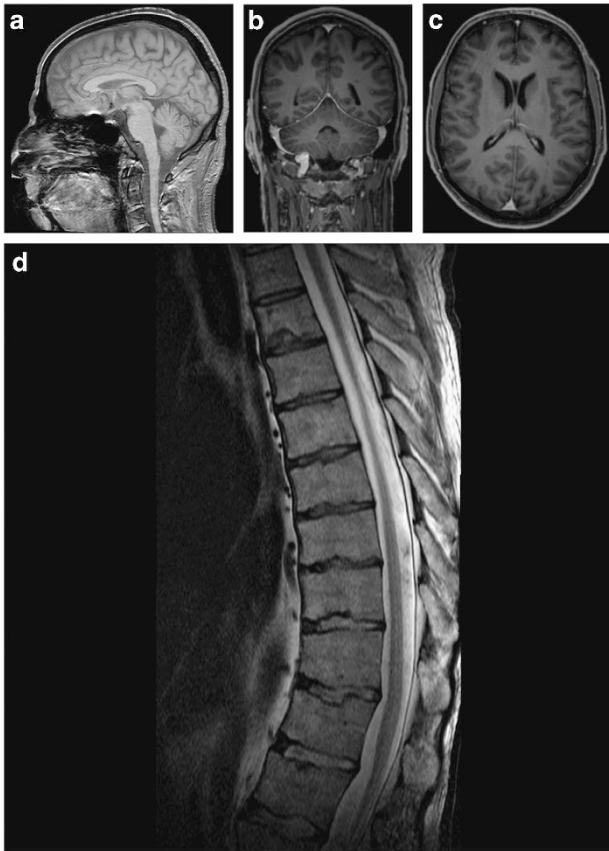
Figure 2. (a–d) Magnetic resonance images of the head and thoracic spine. Cerebral MRI (sagittal T1 weighted (a), coronal (b) and transversal (c) post-gadolinium T1-weighted images) merely shows discrete signs of leukoencephalopathy but no contrast agent enhancement, whereas spinal MRI (sagittal T2-weighted images of the thoracic spine (d)) reveals a reduced bone marrow signal without myelopathy signal and without contrast agent enhancement. The cervical and thoracic cords appear atrophic with an anteroposterior diameter of 5–6 and 4–5 mm, respectively. On the sagittal T2 images, no definitive hyperintense areas are visible.

but should have been taken into further consideration. The absence of elevated protein in cerebrospinal fluid (CSF) and slightly improved values of electroneurography compared with baseline ruled out a Guillain–Barré syndrome or a chronic inflammatory demyelinating neuropathy. The severe peripheral nerve damage impeded clear interpretation of the results of tibialis SSEPs. CD4+ and CD8+ cell counts showed the lowest values when considering the trend since diagnosis of HIV infection. Owing to the heightened risk for opportunistic diseases such as Pneumocystis jiroveci or Mycobacterium avium complex infections, prophylactic antibiotic drug treatment with trimethoprim, sulfamethoxazole and azithromycine was started.

The results so far do not provide a satisfactory explanation for the patient's symptoms and reinforce the necessity of a closer look to a possible para-/infectious myelitis or myelopathy despite a lacking MRI correlate and a normal cell count in CSF.

In this special case, besides common neurotropic viruses, borrelia species, listeria and treponema pallidum, one should give special consideration to the JC virus, a co-infection with HTLV1 or HTLV2, BK virus and the HIV itself.

A CSF sample and blood samples were sent to reference laboratories. IgM, IgG and PCR for HSV, VZV, EBV, CMV, enteroviruses, borrelia, listeria, treponema pallidum, HTLV 1+2, JC and BK virus were negative. HIV-virus load in blood serum reduced adequately after initiation of HAART months ago and was stable below the detection limit of 1.6 log copies per ml, whereas HIV-RNA in CSF showed a distinct increase from 2.01 to 4.0 log copies per ml (Figure 1b).

Having excluded possible structural, ischemic, neoplastic, and parainfectious etiologies and side effects of medication, a potential direct infectious process remains possible (see Table 1 for a summary of the potential differential diagnoses). In this case of an immunosuppressed patient, the HIV itself must be considered as the cause of vacuolar myelopathy. The slight cognitive symptoms mentioned above might also be a sign of an incipient HIV-associated neurocognitive disorder, which commonly parallels HIV-associated myelopathy. Taking the latter into consideration and facing the discordant high virus load in CSF, HAART was adjusted and zidovudine (Antiretroviral CNS Penetration-Effectiveness Score 4) was added to the current regimen in order to maximally suppress HIV replication in the CNS, although the association of vacuolar myelopathy and a productive HIV infection within the spinal cord is not mandatory. Consecutive rehabilitation brought slight motor improvement to the patient, implying a better postural control and an increasing amount of moving along with a wheeled walker; but in general, symptoms remained unchanged.

We certify that all applicable institutional and governmental regulations concerning the ethical use of human volunteers were followed during the course of this research.

DISCUSSION

As HAART has become available as an effective weapon against the HIV, the entity of Neuro-AIDS as the heralding manifestation has changed in the past years to the effect that opportunistic infections and HIV dementia decreased, whereas HIV-associated neurocognitive disorders and HIV-related sensory polyneuropathy still remain common.

Autopsy reports show that HIV-associated myelopathy occurs in ~ 22–55% of HIV/AIDS cases, in which clinical prevalence seems to be much lower, most likely due to underdiagnosis.[1] The disease is characterized by slowly progressive painless spastic paraparesis with sensory ataxia and neurogenic bladder dysfunction. Thoracic spinal cord shows distinct vacuolar histological changes in the ascending and descending tracts, with abnormal MRI findings including spinal cord atrophy (thoracic cord with or without cervical cord involvement), followed by intrinsic cord signal abnormalities, and normal-appearing cord[2]. It has to be clearly distinguished from HIV-associated transverse myelitis in the course of an acute HIV infection (seroconversion) featuring contrast-enhancing intramedullary MRI lesions.[1] Besides spinal epidural lipomatosis as an extremely rare variant of HAART-associated lipodystrophy and the potential of B-cell ablative therapy to trigger or exacerbate CNS inflammatory demyelinating disease, both neoplastic and chemotherapy-induced myelitis could have led to the symptoms in hand. Indeed, the latter was a very unlikely circumstance because of the chronology of the symptoms, as intrathecally administered chemotherapy is known to cause spinal cord lesions at a median of 10 days.[3]

Negative contrast-agent-enhanced MRI sequences of the entire neuro-axis in synopsis with the lack of clinical and laboratory signs of concomitant infectious agents such as bacterial, fungal or parasitical pathogenic organisms do not exclude an infectious myelopathy. It has to be taken into consideration when a patient suffers from HIV infection, especially as—as in this case—the immune system is potentially compromised through immuno-suppressive therapy. Whereas picornaviruses, flaviviruses and rhabdoviruses as characteristic viral pathogens with increased numbers of nucleated cells in CSF cause mainly acute flaccid paralysis, herpes viruses lead to mixed transverse myelitis with or without radiculitis. In ~ 30–60% of cases, acute transverse myelitis is induced by parainfectious mechanisms usually 2–4 weeks after
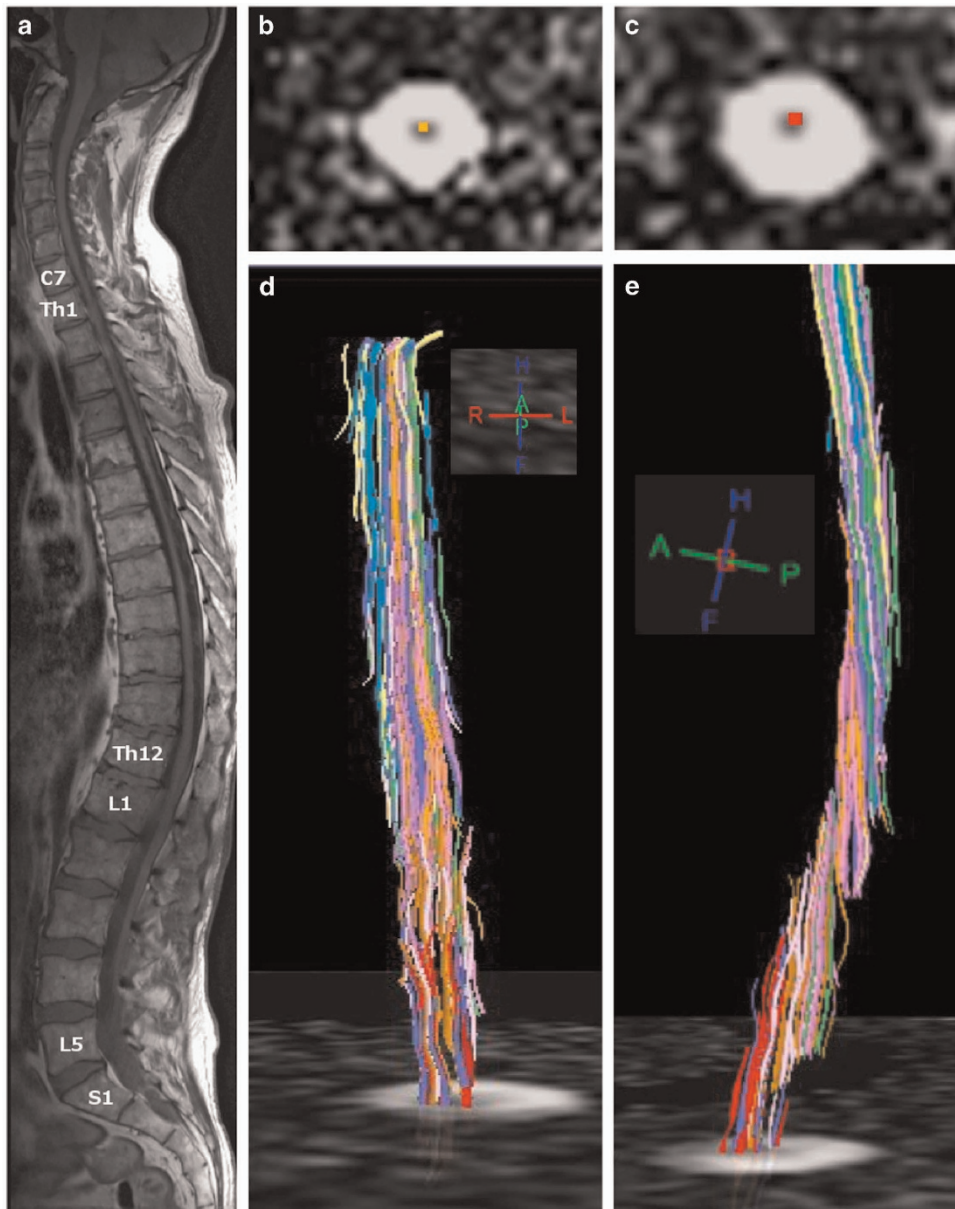
Figure 3. (**a–e**) Magnetic resonance images and tractography of the whole spine (data collection within the follow-up one and a half years later). As an overview, sagittal post-gadolinium T1-weighted spectral presaturation with inversion recovery (SPIR) sequences of the whole spine were performed (**a**). The diffusion tensor imaging and tractography study was performed on a whole-body 3.0-T scanner (Achieva, Philips Medical Systems, Best, Netherlands). Diffusion tensor (DT) images were obtained using a DwiSE scan technique with the following parameters: TR/TE = 3823.4 ms/83.3 ms; flip angle 90°; field of view (FOV) 224 mm; number of signals averaged (NSA), two; 32-noncollinear diffusion gradient directions; b-values, 0 and 800 s mm^{-2}; isotropic voxel size of 2 mm; SENSE technique; spine coil. Sixty slices of DT images on the axial plane were acquired from the mid of the Th7 spine level to the inferior line of Th10. Post-processing analysis was performed on a Philips Extended MR Workspace R2.6.3.1 (Philips Medical Systems, Hamburg, Germany). The Philips FiberTrack package permits streamline tractography with single and multiple regions of interest (ROIs). Algorithm settings are as follows: minimum FA 0.15; maximum angle change (deg) 27.0; and minimum fiber length 10 mm. We performed streamline ('deterministic') tractography with single and multiple regions of interest in the spinal cord. This technique is based on the FACT (fiber assignment by continuous tracking) algorithm, which, in short, connects the largest eigenvectors (with the largest eigenvalue) of the diffusion ellipsoid of the voxels of the spinal cord according to the algorithm setting. The results are streamlines, which depict the main diffusion direction ('axonal direction'). We did not measure the two minor eigenvalues of the diffusion ellipsoid; therefore, no specific information about 'myelination' is available. Three-dimensional single ROI tractography in the anterior and lateral view from thoracic level 7 to 10. At thoracic vertebral level 7, one voxel could be placed into the ADC-map of the spinal cord with an FA value of 0.724 and an ADC of 0.744 × 10-3 mm2/s (**b**). At thoracic vertebral level 8, one voxel could be placed somewhat excentrically into the spinal cord with an FA value of 0.764 and an ADC of 0.741 × 10^{-3} mm^2 s^{-1} (**c**). The lower portion of the spinal cord appeared too small and distorted to place a voxel centrally. Geometric distortion did not allow an exact superposition of the axially reconstructed FA maps on anatomical images. To summarize, the diffusion tensor imaging shows many streamlines in the longitudinal direction of the spinal cord, connecting anisotropic voxels, and did not reveal severe disruptions, but was somewhat degraded by step artifacts due to susceptibility effects, motion and geometric distortion (**d, e**).

Table 1. Differential diagnoses with symptoms and the necessary diagnostic steps

Differential diagnosis	Symptoms	Diagnostic steps
Intraspinal expansive lesion	Subacute spastic paraparesis	Spinal+cerebral MRI, SSEPs
Myelitis/myelopathy	Subacute spastic paraparesis	Contrast-enhanced spinal MRI, lumbar puncture (including neurotropic viruses and bacteria), screening for malignoma, SSEPs
Guillain–Barré syndrome/chronic inflammatory demyelinating polyneuropathy	Progressive polyneuropathy with sensory ataxia	Electroneurography/electromyography, lumbar puncture
Chemotherapy-induced polyneuropathy	Progressive polyneuropathy with sensory ataxia	Electroneurography/electromyography, medical history
Progressive multifocal leukoencephalopathy	Cognitive deficits, subacute spastic paraparesis	Contrast-enhanced spinal+cerebral MRI, JC virus testing, neurocognitive testing
Funicular myelosis	Subacute spastic paraparesis	Holotranscobalamine, methylmalonic acid, homocysteine, vitamin B12, spinal MRI
HAART-associated spinal epidural lipomatosis	Subacute spastic paraparesis, back pain	Spinal MRI

Abbreviations: CSF, cerebrospinal fluid; HAART, highly active antiretroviral treatment; HAND, HIV-associated neurocognitive disorder; JC virus, John Cunningham virus; MRI, magnetic resonance imaging; PML, progressive multifocal leukoencephalopathy; SSEP, somatosensory-evoked potentials.

acute infection. However, chronic spastic paralysis is found with retroviruses such as HTLV-1/2 and the HIV.[4] As in the present case, detailed analysis of serum and CSF did not unveil any other pathogenic organism, the one to remain is the HIV. It is well known from the literature that blood and CSF viral populations may diverge functionally and genetically during chronic HIV infection. CSF HIV viral load in this patient was markedly elevated in comparison with the values at the time point of HIV-vacuolar myelopathy diagnosis and clearly differed from suppressed viral load in the serum. According to the sparse literature available postulating that viral load in CSF is not related to the presence and severity of vacuolar myelopathy, the constellation of laboratory findings in this case cannot be used as hard criterion for the latter diagnosis. To escalate the HAART therapy with medications having a higher CNS penetration-effectiveness index as individual therapeutic attempt seems to be the only logical step, particularly in view of the fact that some reports suggest functional and clinical improvement[5], whereas L-methionin and intravenous immunoglobulin failed to show any positive effects in HIV-associated myelopathy.

One and a half years later, the patient's neurological status was found to remain stable. We performed a diffusion tensor image study on a whole-body 3.0-T scanner, which revealed many streamlines in the longitudinal direction of the spinal cord, connecting anisotropic voxels, and did not reveal severe disruptions, but was somewhat degraded by step artifacts due to susceptibility effects, motion and geometric distortion (Figures 3d and e). Nevertheless, fractional anisotropy maps with color encoding showed many areas in bright blue along the course of the atrophic thoracic spinal cord, reinforcing that the principal direction of the diffusion ellipsoid is longitudinal and not purely an artifact. It is interesting that despite the atrophy of the spinal cord there is sufficient directional anisotropy with a large amount of reconstructable fibers in the longitudinal direction. This finding may be linked with the reported histologic finding of vacuolar myelopathy demonstrating no significant axonal loss in areas of vacuolation.[1]

To summarize, this case points out several important issues. First, when diagnosing HIV-positive patients with clinical signs of myelopathy, a negative or unspecific MRI scan excludes possible differential diagnoses but by no means rules out structural and functional damage of the myelon. Furthermore, the presence of spinal cord atrophy supports the diagnosis of vacuolar myelopathy. Moreover, to our knowledge, these are unique pictures of a patient's spinal tract with HIV-associated myelopathy, revealing the radiologic correlate of no significant spinal axonal loss as a histopathologic finding. Second, SSEPs may be of limited use because of impaired peripheral nerve conduction. Third, precise screening for a (para-)infectious etiology is mandatory, but one should be aware that the HIV itself is very likely associated with the neurological disease ('Entities should not be multiplied unnecessarily', William Ockham, 14th century). Finally, peripheral and central viral load should always be assessed to avoid missing a possible 'CSF HIV-escape'.

COMPETING INTERESTS
The authors declare no conflict of interest.

REFERENCES
1 Dal Pan GJ, Glass JD, McArthur JC. Clinicopathologic correlations of HIV-1-associated vacuolar myelopathy: an autopsy-based case-control study. *Neurology* 1994; **44**: 2159–2164.
2 Chong J, Di Rocco A, Tagliati M, Danisi F, Simpson DM, Atlas SW. MR findings in AIDS-associated myelopathy. *AJNR Am J Neuroradiol* 1999; **20**: 1412–1416.
3 Kwong Y-L, Yeung DYM, Chan JCW. Intrathecal chemotherapy for hematologic malignancies: drugs and toxicities. *Ann Hematol* 2008; **88**: 193–201.
4 Cho TA, Vaitkevicius H. Infectious myelopathies. *Continuum (Minneapolis Minn.)* 2012; **18**: 1351–1373.
5 Bizaare M, Dawood H, Moodley A. Vacuolar myelopathy: a case report of functional, clinical, and radiological improvement after highly active antiretroviral therapy. *Int J Infect Dis* 2008; **12**: 442–444.